Analyzing tactical control strategies for aircraft arrivals at an airport using a queuing model

Itoh, Eri; Mitici, M.A.

DOI
10.1016/j.jairtraman.2020.101938

Publication date
2020

Document Version
Accepted author manuscript

Published in
Journal of Air Transport Management

Citation (APA)
Itoh, E., & Mitici, M. A. (2020). Analyzing tactical control strategies for aircraft arrivals at an airport using a queuing model. *Journal of Air Transport Management*, *89*, Article 101938. https://doi.org/10.1016/j.jairtraman.2020.101938

Analyzing tactical control strategies for aircraft arrivals at an airport using a queuing model

Eri Itoh[a,c], Mihaela Mitici[b]

[a] *Air Traffic Management Department, Electronic Navigation Research Institute, 182-0012 Tokyo, Japan*
[b] *Faculty of Aerospace Engineering, Delft University of Technology, HS 2926 Delft, The Netherlands*
[c] *Department of Aeronautics and Astronautics, School of Engineering, The University of Tokyo*

Abstract

This paper proposes to analyze control strategies for arrival air traffic at an airport using a classical queuing model. The parameters of our model are estimated by means of a data-driven analysis of two years of radar tracks and flight plans for arrival flights at Tokyo International Airport from 2016 and 2017. Our results show that increasing the capacity with one or two more aircraft in the airspace up to 60 NM around the airport significantly mitigates arrival delays, even when assuming future, increased arrival traffic volumes. The outcomes of this study provide insights into the effectiveness of arrival control strategies and are seen as a means to recommend scenarios to be further analyzed with human-in-the-loop simulations.

Keywords: queuing theory, data analysis, stochastic, extended arrival management, air traffic management

1. Introduction

The management of aircraft arrivals at airports is central to airport operations. In the United States, Traffic Management Advisory (TMA) (7) was deployed in air traffic control centers in the 1990's, while its enhanced version, Time-Based Flow Management (TBFM) (9) and Terminal Sequencing and Spacing (TSAS) (20), takes into account future airborne-based operations (21). These systems contribute to sequencing and time-spacing of the arrival traffic consistently in the en-route and terminal airspace areas. In Europe, the on-going SESAR project has facilitated collaboration among European countries and contributed to the development of "Enhanced" Arrival Management (AMAN), which coordinates the arrival time-schedules covering wider ranges of airspace than in the case of conventional operations (8). In Asia-pacific, targeting strategic air traffic flow management, Long Range Air Traffic Flow Management (LRATFM) has been devised to provide a basis for research into applications beyond current system time-frames (13). On-going Japanese research and development on the "Extended" AMAN (E-AMAN) aims to ensure efficient arrival traffic flow at Tokyo International Airport (14). In the E-AMAN scheme, arrival traffic flow control, which coordinates traffic volume under limited airspace capacity and runway throughput, shifts to time-based operations close to the destination airports, which ensures minimum time-spacing between arrivals. An efficient transition from flow control to time-based operations depends on the characteristics of the arrival air traffic flow and its surrounding environment, such as, the runway and airspace capacity, weather conditions, air routes or geographical constraints. One of the most important requirements for the design of future Air Traffic Management (ATM) system is to accommodate an increase of 250% in the global air traffic in the next 20 years, while reducing airport arrival delay (12).

Several studies have analyzed the aircraft arrival process at airports by means of queuing theory. The aircraft arrival delay is analyzed in (4; 6; 19; 5) by employing queuing models focused especially on runway-related delay and capacity constraints. In (4), the expected waiting time for aircraft arriving in a single runway is determined using an $M/SM/1$ queuing model. Simple bounds for the expected waiting time are determined by comparison to $M/G/1$ and $M/D/1$ models. However, in their case study, the authors do not make use of operational data or compare their results against actual data. In (19), the arrival of aircraft at Pittsburgh International Airport is modelled as an $M/M/1$ and $M/E_k/1$ queue. The authors determined, using Semi-Markov decision processes, the maximum number of aircraft allowed to land at the airport during peak hours. In (5), the expected aircraft

arrival delay was estimated by means of $M/D/n$ queues, which yielded reasonable results when compared with numerical simulation data. Again, no comparative analysis with actual flight data was conducted. In (6), the National Airspace System in USA is modelled as a network of aircraft arriving, taxiing and departing queues, where the TRACON sectors are modelled as an $M/E_3/n$ queue. A macroscopic view of the impact of ATM technologies and costs is provided. A microscopic analysis of traffic using queuing theory is provided in (10; 18), where flows of pedestrians are modelled. In (10), an $M/G/c/c$ queue is proposed to model road traffic. The results show that the model captures well the characteristics of the road traffic. In (15) an $M/G/c$ queuing model is proposed to analyze air traffic in an airspace around an airport. In (16), a discussion on future air traffic control strategies is provided. In (18), a state dependent $M/M/c/K$ queuing model is applied to control the pedestrian flows and the capacity of pedestrian facilities in open outdoor walking environments.

In this study we propose to analyze arrival air traffic under current and novel traffic control strategies using a classical queuing model. In particular, we conduct a macroscopic analysis of the aircraft arrival traffic at an airport using a classical $M/G/c/K$ queuing model. We determine the model parameters using 2 years of flight plans and track data at Tokyo International Airport. We first estimate the expected arrival delay under the current tactical arrival management strategy, for increasing aircraft arrival rates. Second, we analyze additional tactical arrival strategies, such as increasing the airspace capacity closer to the airport or adjusting the flight time in specific airspace areas. Our results show that a slight increase in the airspace capacity results in much lower arrival delays than when adjusting the flight times. The outcomes of this study contribute to the design of arrival management systems and control strategies to be used by air traffic controllers at an airport. Equally important, our approach provides insights into the effectiveness of arrival control strategies and is seen as a means to recommend scenarios to be further analyzed with human-in-the-loop simulations.

The paper is organized as follows. Section 2 introduces air traffic operations at Tokyo International Airport, and characterizes the arrival traffic data recorded in 2016 and 2017. This data analysis supports the models presented in this paper. Section 3 proposes a queue-based modeling approach where the aircraft arrival process is formulated as a $M/G/c/K$ queuing model. Based on the data-driven analysis, probability distributions of the inter-arrival time and service time, and the number of service counters are estimated. In Section 4, the $M/G/c/K$ queuing model is applied to estimate the aircraft arrival delay time as a function of the distance away from the airport. The estimation results allow us to analyze the relation among arrival rate, airspace capacity, and aircraft waiting time (arrival delay time). Section 5 clarifies efficient arrival control strategies based on the estimation results of arrival traffic delay while increasing arrival ratio and airspace capacity, and adjusting means of service times using the $M/G/c/K$ queuing model. Section 6 discusses how this proposed queue-based approach contributes to the design of future operational procedures and technologies, combined with the results of the $G/G/c$ queuing approach. Additionally, authors' future works on mathematical modeling of the aircraft arrival process are discussed, as well as further extensions of the study. Finally, Section 7 presents the conclusions of this study and outlines our plans for future work.

2. Data description for case study - Tokyo International Airport

2.1. Aircraft arrival operations

This section provides a description of the aircraft arrival operations at Tokyo International (Haneda) Airport. Tokyo International Airport is the 5th busiest airport in the world with respect to passenger traffic, having a total of 83,189,933 passengers in 2017. An increase of 4.32% in the number of passengers was registered in 2017 relative to 2016 (1). A maximum number of 447,000 departures and arrivals are accommodated per year, with a maximum of 80 operations in one hour. Over 60% of the domestic flights in Japan are concentrated at this airport. The airport makes use of four runways on a daily basis, while the choice of the runway configuration depends on wind direction (see Figure 1). For the north wind operations, runway 34L is used for arrivals from the south-west direction, while runway 34R is used for arrivals from the north. Runway 34R is also used for departure traffic. For south wind operations, runway 22 is used for arrivals from the south-west, and runway 23 for arrivals from the north.

The case study in this paper is based on flight plans and track data for a period of 71 days, which are randomly selected from the odd months of 2016 and 2017. In 2016, there are a total of 608 arrivals per day, of which 530 flights

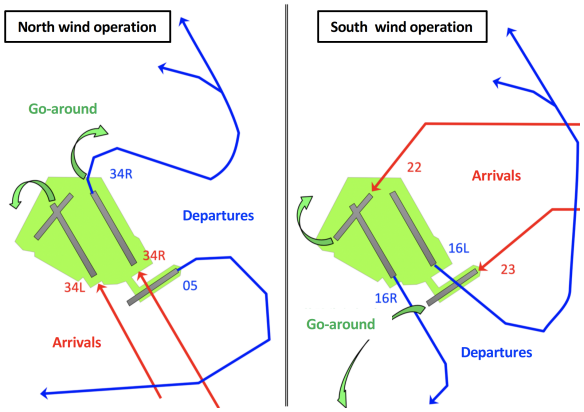

Figure 1: Departure and arrival operations depending on wind direction.

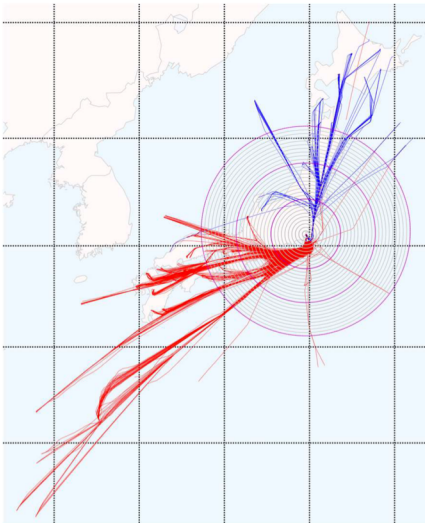

Figure 2: Example of flight tracks during an entire day in November 2016. The red tracks show the south-west traffic flow. The blue tracks show the north traffic flow.

are domestic and 78 flights are international. In 2017, 8 additional international flights are accommodated every day compared to 2016. Thus, in 2017, there are a total of 614 arrivals per day, of which 530 flights are domestic and 84 flights are international. The total number of arrivals between 8:00 AM and 11:00 PM is slightly below the maximum allowed daily traffic thresholds, while the most congested period is between 5:00 PM and 10:00 PM.

Table 1 shows the type of aircraft, in percentage, used for the arrivals/departures. The majority of the aircraft are used for short and medium-distance passenger transportation using A737-800 (B738), A320, and B767-300 (B763). Secondly, long-distance passenger aircraft such as B777-200 (B772) and B787-8 (B788) are used. Finally, less than 1% of the flights are business jet including Gulfstream and Bombardier products.

One of the features of the arrival traffic flow at Tokyo International Airport is that the arrivals are clustered either in the north or the south-west part of the airport. In the period 8:00 AM-11:00 PM, there are a total of 569 arrivals, of which 422 flights arrive from south-west, and 147 flights arrive from north. Figure 2 shows flight track data for one day of operation in November 2016. The flight tracks of arrivals that use runway 34L are drawn in red, while arrivals in runway 34R are drawn in blue. Concentric circles are drawn every 10 NM radius, from 10 NM to 300 NM, centered at Tokyo International Airport.

Figure 3 shows the hourly number of flights arriving from south-west or north in the period 8:00 AM-11:00 PM.

Table 1: Percentage of aircraft types out of the total aircraft arrivals.

Types	B738	B763	B772	A320	B788	B773	B77W	B789	A321	B737	A333	E170	A332	B744	B734	Others
(%)	34	18	14	10	6	3	3	2	2	2	2	1	0.6	0.5	0.4	0.8

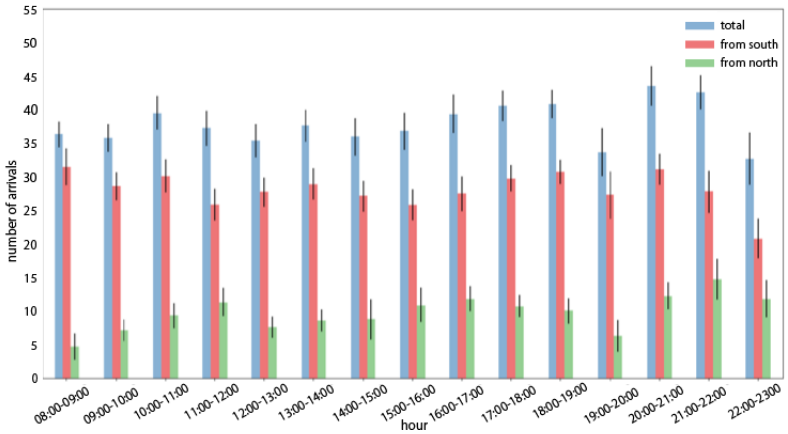

Figure 3: Mean and STD of hourly number of arrivals from south-west (red) and north (green) in the period 8:00 AM-11:00 PM.

It can be seen that the number of arrivals from south-west is approximately three times larger than the number of arrivals from the north. In the near future, the number of arrivals from south-west is expected to grow as a result of an increasing Asian traffic demand (12).

Air traffic flow in Japan is strategically controlled with a central focus on arrivals at Tokyo International Airport. Figure 4 shows the number of arrival flights crossing every concentric circle (see also Fig. 2) in an hour from 5:00 PM to 10:00 PM. The total number of flight arrivals are controlled within a maximum of 40 (30 times from the south-west, 10 times from the north).

3. Model description and formulation of the aircraft arrival traffic

3.1. Model description and formulation of the aircraft arrival process as a M/G/c/K queue

We formulate the aircraft arrival process by means of a $M/G/c/K$ queuing model as follows. We consider the airspace area around the airport located between concentric circles of radius 20 NM-150 NM, 40 NM-15 0NM, 60 NM-150 NM, 80 NM-150 NM, 100 NM-150 NM, and 150 NM-300 NM, as shown in Figure 5. As a result, there are 6 airspace areas $i = 1, 2, \ldots, 6$, where area $i = 1$ is the airspace area around the airport from 20 NM to 150 NM radius, area $i = 2$ is the airspace area around the airport from 40 NM to 150 NM radius, and so on.

Each of the airspace area $i, 1 \leq i \leq 6$, is modelled as a $M/G/c/K$ queue, where aircraft arrive at airspace $i, 1 \leq i \leq 6$, according to a Poisson process with rate λ_i. The arrivals are separated in distance for safety reasons. The time interval between two consecutive arrivals at an airspace area $i, 1 \leq i \leq 6$ is called the aircraft inter-arrival time (see Fig. 5). Upon arrival, the aircraft receives service for a certain amount of time, i.e., the time the aircraft spends flying the given airspace (see Fig. 5). We assume that the aircraft service times are independent and identically distributed according to a general distribution with finite mean. Let $\mathbb{E}[B_i]$ denote the expected service time of an aircraft in airspace area $i, 1 \leq i \leq 6$, i.e., the time an aircraft flies airspace area i. We assume that the service time for an aircraft in an airspace area i is $\mathbb{E}[B_i] = D/v$, where D is the distance an aircraft is flying and v is the average speed at which the aircraft is flying this distance. For an airspace $i, 1 \leq i \leq 6$, we consider c_i servers, which indicates the number of aircraft that are allowed to be present at any time in the given airspace, i.e., the capacity of the given airspace. We also consider a buffer of size K_i, which indicates the maximum number of aircraft allowed to be present in airspace i and that receive service. If already c_i aircraft are present in airspace area i, then $K_i - c_i$ aircraft are still allowed to be present in airspace i and will receive service at a later time. If, however, the number

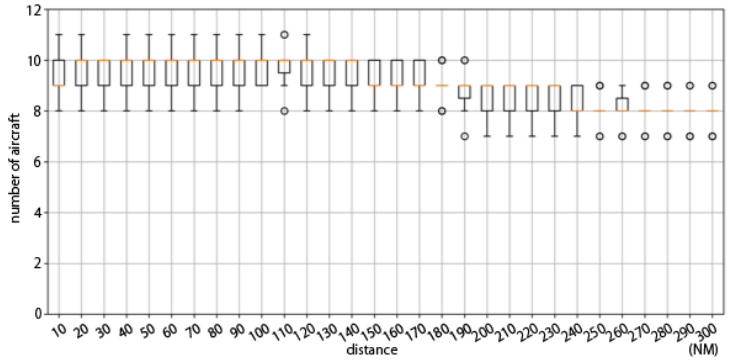

(a) North traffic flow.

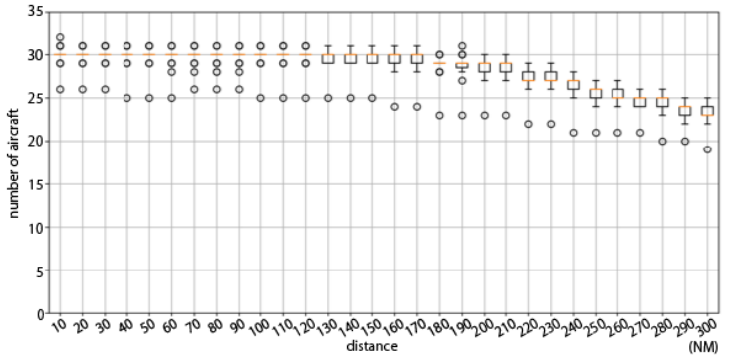

(b) South traffic flow.

Figure 4: Number of aircraft arrivals in an hour during 5:00 PM-10:00 PM in 2016 and 2017.

Table 2: Parameters of empirical distributions of the inter-arrival time in seconds.

Radius around the airport (NM)	30	100	150	300
$\mathbb{E}[A_i]$ (sec)	112.4	106.3	107.0	135.8
$\sigma_[A_i]$ (sec)	623.3	4723	7494	12168
$C_e[A_i]$	0.03810	0.4182	0.6544	0.6603

of aircraft at airspace area $i, 1 \leq i \leq 6$ has already reached the buffer size K_i and additional aircraft would like to make use of airspace i, then these additional aircraft are blocked from the system.

In the next section we establish the choice of our modeling approach by means of a flight data analysis.

3.2. Data-driven parameter estimation of the $M/G/c/K$ model for aircraft arrival traffic

Our modeling approach in Section 3.1 is motivated by a data-driven analysis based on the flight plans and radar data corresponding to the arrival aircraft in 2016 and 2017 at Tokyo International Airport. We consider the time period of 5:00 PM to 10:00 PM, which is the most congested arrival part of the day at Tokyo International Airport.

Figure 6 shows the empirical probability densities of aircraft inter-arrival times where the arrivals cross concentric circles around the airport of radii 30, 100, 150 and 300 NM, against their exponential fittings. The results show that the aircraft inter-arrival time distributions at 150 NM and 300 NM radius around the airport are well approximated by an exponential distribution. However, the inter-arrival times converge to a nearly Gaussian distribution closer to the arrival airport.

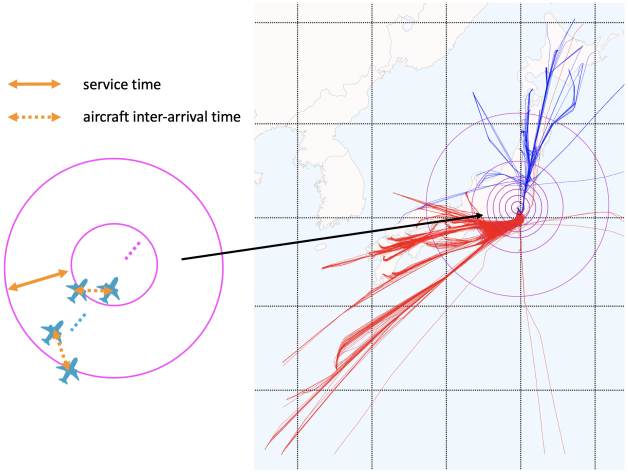

Figure 5: Illustration of the service time and inter-arrival time with 6 airspace areas.

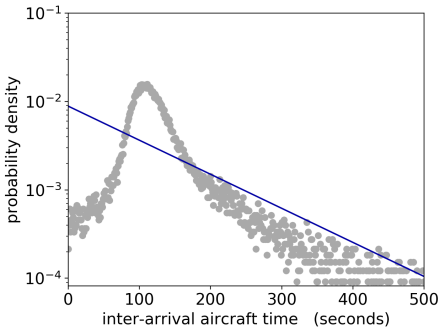

[1] Aircraft inter-arrival times - 30 NM radius around the airport.

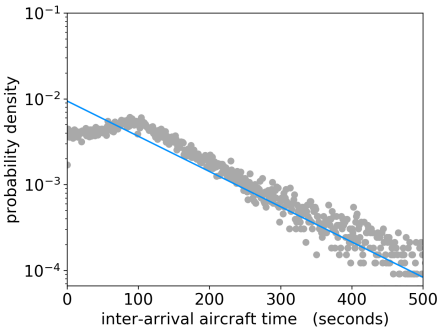

[2] Aircraft inter-arrival times - 100 NM radius around the airport.

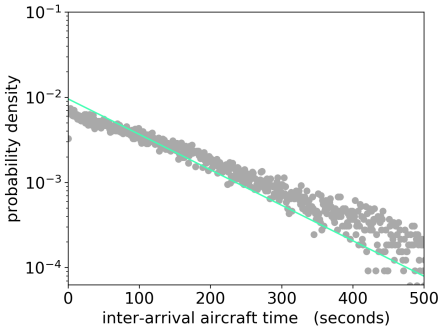

[3] Aircraft inter-arrival times - 150 NM radius around the airport.

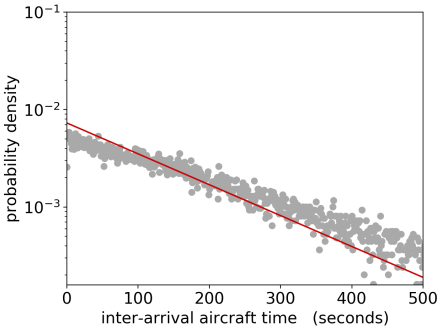

[4] Aircraft inter-arrival times - 300 NM radius around the airport.

Figure 6: Distribution of inter-arrival time with exponential fitting.

In Table 2, the coefficient of variance of inter-arrival times in airspace area $i, 1 \leq i \leq 6$, denoted by $C_e[A_i]$, is

defined as:

$$C_e[A_i] = \frac{\sigma_{A_i}}{\mathbb{E}[A_i]^2}, \tag{1}$$

where $\mathbb{E}[A_i]$ and σ_{A_i} are, respectively, the mean inter-arrival time and the variance of the inter-arrival time in airspace i. When $C_e[A_i] \to 1$, the empirical distribution of the inter-arrival time is well approximated by an exponential distribution.

Figure 7 shows the empirical distributions of the service times corresponding to the airspace area $i \in \{1,2,\ldots,6\}$. Figure 8 shows the number of aircraft flying in the airspace area $i \in \{1,2,\ldots,6\}$ at a fixed moment every 10 minutes during the time period of 5:00 PM to 10:00 PM, and the corresponding mean and standard deviation (STD) are given in Table 3. Following the analysis of the flight data (see also Fig.8 and Table3), in this paper, we estimate the number of servers c_i in airspace area $i, 1 \le i \le 6$, as the mean number of aircraft present in airspace i plus 2STD of the number of aircraft, i.e., for 95% of the time, in airspace area i, at most c_i aircraft can be handled at the same time. This constraint reflects the capacity constraints imposed on the aircraft arrival airspace.

Following the analysis of the flight plans and track data analysis (see also Tab.4), Table 4 shows the estimates of the $M/G/c/K$ model parameters λ_i, arrival ratio per second, and $\mathbb{E}[B_i]$, the mean of service time, for airspace area $i, 1 \le i \le 6$. We also consider a buffer K_i for each area $i, 1 \le i \le 6$, such that a maximum of K_i, aircraft are allowed to be present in airspace area $i, 1 \le i \le 6$, at the same time. The size of buffer K_i is determined by constraining the probability of blocking aircraft in airspace i, which we denote by p_{K_i}, to be below 0.01, where it is known that (2; 11):

$$p_{K_i} = \frac{(\lambda_i \mathbb{E}[B_i])^{K_i}}{c_i! c_i^{K_i - c_i}}.$$

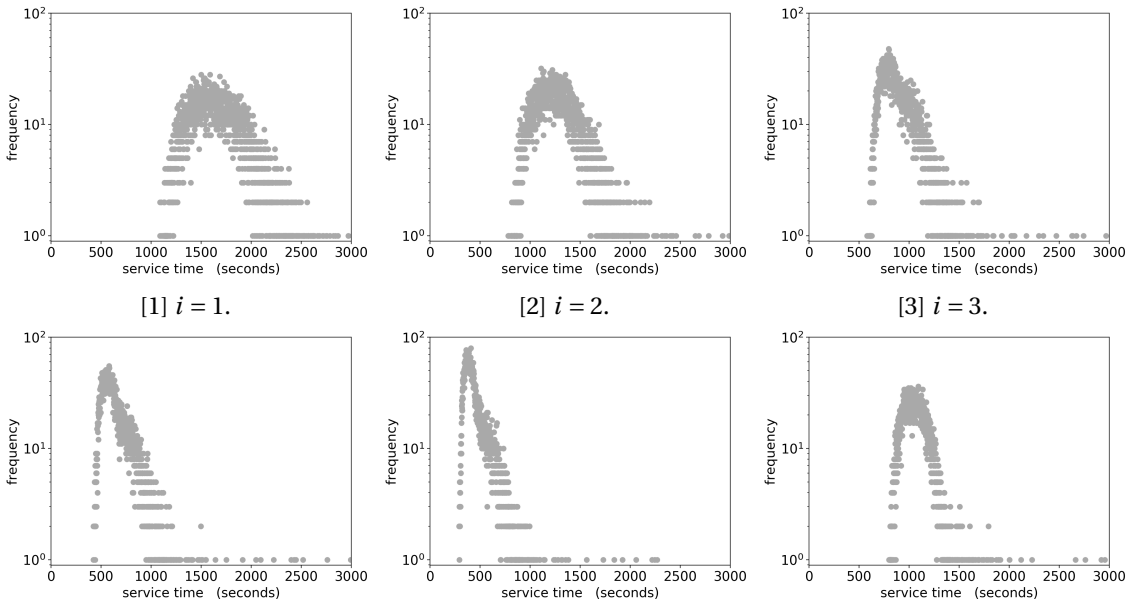

[1] $i = 1$. [2] $i = 2$. [3] $i = 3$.

[4] $i = 4$. [5] $i = 5$. [6] $i = 6$.

Figure 7: Empirical service time distribution for airspace area $i, 1 \le i \le 6$.

Table 3: Estimating the number of servers c_i in airspace area $i, 1 \le i \le 6$.

Airspace area i	1	2	3	4	5	6
Empirical mean number of aircraft	13.90	10.67	7.498	5.487	3.800	9.231
Empirical STD number of aircraft	2.598	2.287	2.075	1.886	1.674	2.305
Estimated number of servers c_i	20	17	13	10	8	16

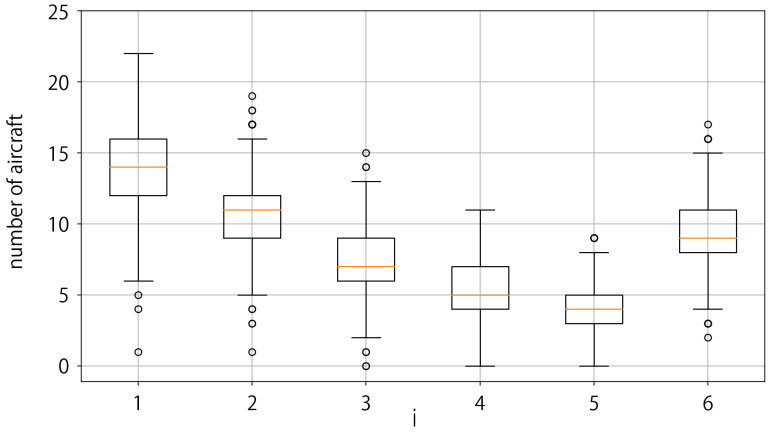

Figure 8: Number of aircraft present in airspace area $i, 1 \le i \le 6$ averaged over 70 days randomly chosen from 2016 and 2017 over 2 years data.

Table 4: Data-driven parameter estimation for the $M/G/c/K$ queuing model - airspace area $i, 1 \le i \le 6$.

Airspace area i	1	2	3	4	5	6
$\mathbb{E}[B_i]$ (sec)	1640	1254	877.5	634.9	433.0	1055
λ_i (per sec)	0.009345	0.009345	0.009345	0.009345	0.009345	0.007366
K_i	26	21	16	13	10	17

4. Analyzing aircraft arrivals using a $M/G/c/K$ queuing model

4.1. Determining aircraft delay time

For a given airspace i, $p_n(i)$ denotes the probability that there are n aircraft present in that area. It is known that (2; 11):

$$p_n(i) = \begin{cases} \frac{(\lambda_i \mathbb{E}[B_i])^n}{n!} p_0(i), \text{ for } 0 \le n \le c_i \\ \\ \frac{(\lambda_i \mathbb{E}[B_i])^n}{c_i! c_i^{n-c_i}} p_0(i), \text{ for } c_i < n \le K_i. \end{cases} \tag{2}$$

Following normalization, we have:

$$p_0(i) = \left(\sum_{n=0}^{c_i} \frac{(\lambda_i \mathbb{E}[B_i])^n}{n!} + \sum_{n=c_i+1}^{K_i} \frac{(\lambda_i \mathbb{E}[B_i])^n}{c_i! c_i^{n-c_i}} \right)^{-1}. \tag{3}$$

Then, using (2) and (3), the mean queue length in the airspace area i, denoted by $L^q(i)$, is:

$$L^q(i) = \sum_{n=c_i+1}^{K_i} (n - c_i) p_n(i) = \sum_{n=c_i+1}^{K_i} (n - c_i) \frac{(\lambda_i \mathbb{E}[B_i])^n}{c_i! c_i^{n-c_i}} p_0(i). \tag{4}$$

Finally, let $\mathbb{E}[D_i]$ denote the expected delay experienced by the aircraft in the airspace area i, which is absorbed by means of vectoring or speed adjustments. From Little's law (17) and (4), we have:

$$\mathbb{E}[D(i)] = \frac{L^q(i)}{\lambda_i(1-p_K(i))} = \frac{L^q(i)}{\lambda_i\left(1-(\lambda_i\mathbb{E}[B_i])^{K_i}\frac{1}{c!c_i^{K_i-c_i}}p_0(i)\right)}. \tag{5}$$

To illustrate the above derivations by means of an example, we refer to (2), Section 11.2.

4.2. Analyzing required airspace capacity and minimum airspace buffer size to maintain a given level of performance with respect to aircraft arrival delay

Figure 9 shows the relationship between the airspace capacity c_i, arrival traffic rate λ_i, buffer size K_i of airspace i, and arrival delay time $\mathbb{E}[D_i]$ in the airspace area $i, i \in \{1,6\}$. In all the analyzed cases, we ensure that $p_{K_i} < 0.01$. This may mean, for instance, that the size of the buffer K_i or the capacity c_i of the airspace may be adjusted to ensure that the blocking probability remains below 0.01. We also consider the case when the arrival rate λ_i increases with 10% and 20% for the airspace $i, i \in \{1,6\}$.

Overall, Figure 9 captures the characteristics of the aircraft arrival flow and provides insights into the air traffic control strategies needed, i.e., increased capacity or buffer size, to maintain a given level of performance with respect to the arrival delay. Firstly, reducing c_i, i.e., reducing the airspace capacity, $i \in \{1,6\}$, leads to increasing arrival time delay $\mathbb{E}[D_i]$. Moreover, to ensure that p_{K_i} remains below 0.01, the size of the buffer K_i also increases. As expected, further increasing the aircraft arrival rate in airspace $i, i \in \{1,6\}$, only increases the arrival delay. Secondly, increasing the arrival traffic rate $\lambda_i, i \in \{1,6\}$, leads to an increase of $\mathbb{E}[D_i]$ when the number of servers c_i, i.e., the capacity of airspace i, remains the same. This means that the optimal c_i values, which maintain $\mathbb{E}[D_i]$ within the acceptable range, increase according to the traffic volume in airspace i. Thirdly, the airspace $i = 1$ requires more airspace capacity c_i than the airspace $i = 6$. Because the aircraft reduces the airspeed while descending to the destination airport, the air traffic in the airspace $i = 1$ is denser than that in the airspace $i = 6$. Therefore, the capacity c_i in the airspace $i = 1$ is greater than that in the airspace $i = 6$ when aiming to maintain the same level of arrival delay $\mathbb{E}[D_i]$.

Table 5: Expected arrival delay time $\mathbb{E}[D_i]$ and minimum required buffer size K_i such that $p_{K_i} < 0.01, 1 \le i \le 6$.

i		**1 (20-150NM)**	**2 (40-150NM)**	**3 (60-150NM)**	**4 (80-150NM)**	**5 (100-150NM)**	**6 (150-300NM)**
c_i		**20**	**17**	**13**	**10**	**8**	**16**
λ_i	K_i	26	21	16	13	10	17
	$\mathbb{E}[D_i]$ (sec)	14.75	4.914	2.696	2.640	0.8561	0.0
$110\%\lambda_i$	K_i	32	24	19	16	12	18
	$\mathbb{E}[D_i]$ (sec)	58.93	20.10	11.70	9.554	4.462	0.5002
$120\%\lambda_i$	K_i	41	27	20	16	12	17
	$\mathbb{E}[D_i]$ (sec)	179.8	39.12	17.47	12.38	4.26	0.0
$130\%\lambda_i$	K_i	98	34	24	19	13	18
	$\mathbb{E}[D_i]$ (sec)	2483	111.5	38.08	23.44	7.367	0.9706

4.3. Estimating arrival delay under future traffic increase

Future air transport is expected to grow by 250% in the next 20 years (12). Allowable runway throughput can be estimated according to the value of separation minima, which is determined by considering the aircraft's wake vortex category and the automation levels supporting air traffic controllers (3). In this section, we assume a 10%, 20%, and 30% increase in arrival traffic, and discuss the impact of arrival delay against increasing air traffic volumes. The same airspace capacity $c_i, 1 \le i \le 6$ is assumed as in Table 3 in order to analyze the tolerance of the current airspace capacity against increasing traffic demand.

Table 5 shows the expected arrival delay and the minimum required buffer size for airspace $i, 1 \le i \le 6$ for an arrival rate up to 30% more than the current arrival rate. Figure 10 compares the estimated arrival delay time $\mathbb{E}[D_i]$

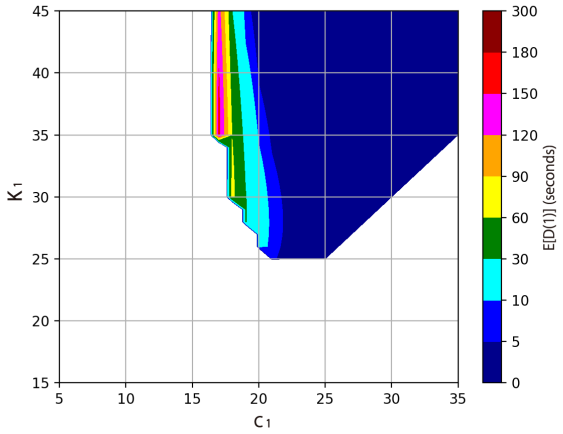

[1] λ_1.

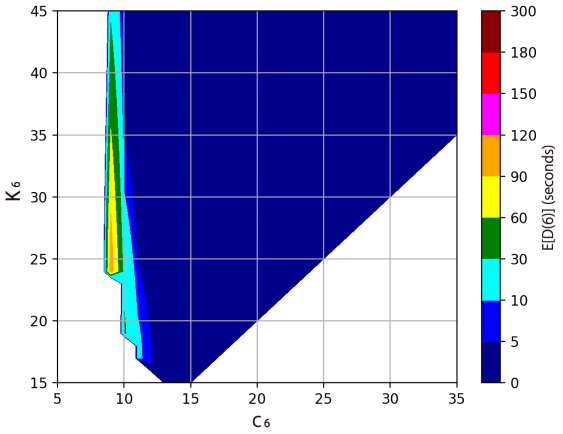

[2] λ_6.

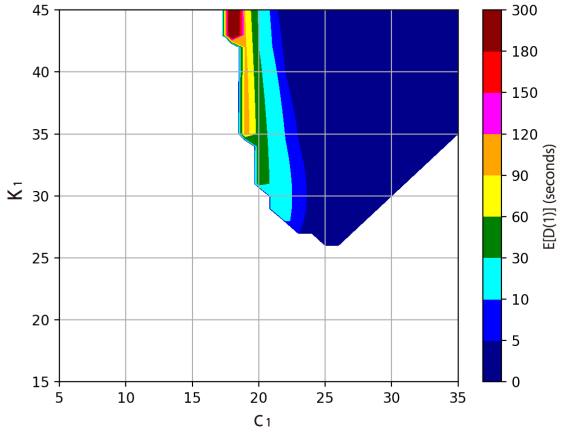

[3] $\lambda_1^* = 110\%\lambda_1$.

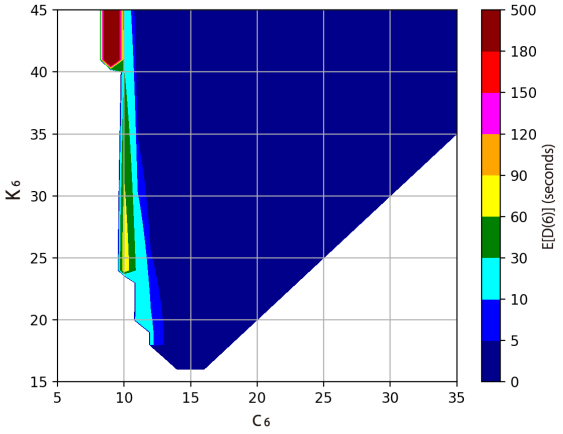

[4] $\lambda_6^* = 110\%\lambda_6$.

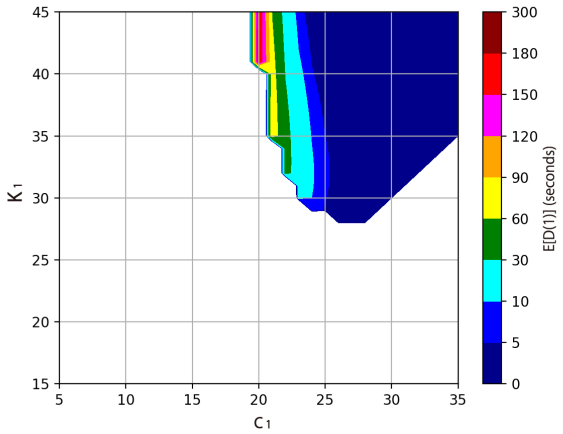

[5] $\lambda_1^{**} = 120\%\lambda_1$.

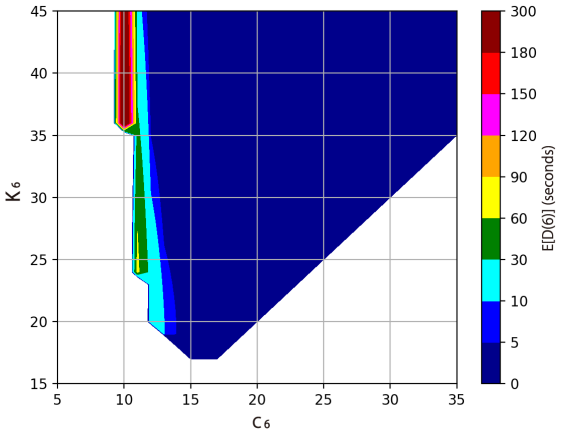

[6] $\lambda_6^{**} = 120\%\lambda_6$.

Figure 9: Comparative analysis of buffer size K_i, number of servers c_i, and expected waiting time $E[D_i]$ when the arrival rate increases with 10% and 20% airspace areas $p_{K_i} < 0.01$, $i \in \{1,6\}$.

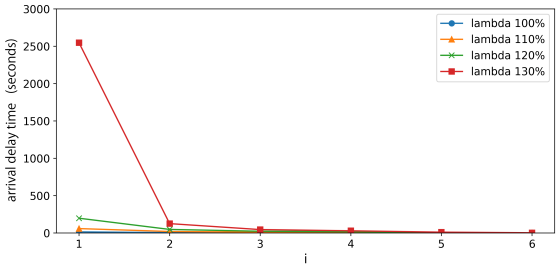

[1] Increasing arrival delay time, $100\%\lambda_i$, $110\%\lambda_i$, $120\%\lambda_i$ and $130\%\lambda_i, i \in \{1,2,\ldots,6\}$.

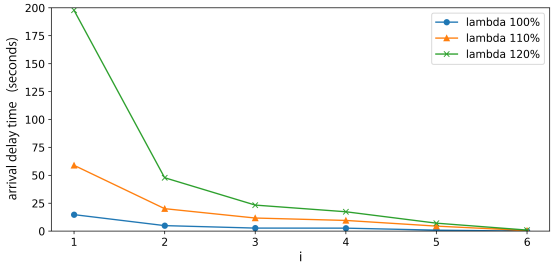

[2] Increasing arrival delay time, $100\%\lambda_i$, $110\%\lambda_i$, and $120\%\lambda_i, i \in \{1,2,\ldots,6\}$.

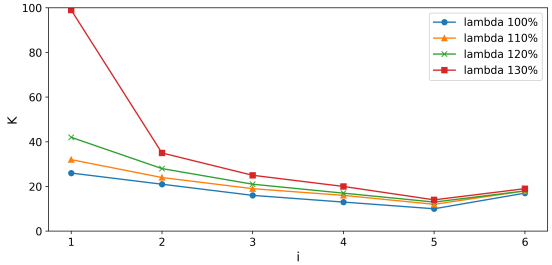

[3] Buffer size K_i estimation under $p_{K_i} < 0.01, i \in \{1,2,\ldots,6\}$.

Figure 10: Comparing arrival delay and the size of the buffer $K_i, i \in \{1,2,\ldots,6\}$, by increasing airspace capacity.

Table 6: Expected arrival delay time $\mathbb{E}[D_i]$ given 110%c_i and the minimum required buffer size K_i such that $p_{K_i} < 0.01, 1 \le i \le 6$.

i		**1 (20-150 NM)**	**2 (40-150 NM)**	**3 (60-150 NM)**	**4 (80-150 NM)**	**5 (100-150 NM)**	**6 (150-300 NM)**
c_i		**22**	**18**	**14**	**11**	**8**	**17**
λ_i	K_i	25	20	16	13	10	18
	$\mathbb{E}[D_i]$(sec)	2.574	1.014	0.7229	0.6654	0.8561	<0.1
110%λ_i	K_i	28	22	17	14	11	18
	$\mathbb{E}[D_i]$(sec)	12.04	5.840	2.561	2.044	2.231	<0.1
120%λ_i	K_i	32	25	19	15	12	18
	$\mathbb{E}[D_i]$(sec)	37.29	18.05	7.331	4.485	4.260	<0.1
130%λ_i	K_i	40	30	21	17	13	18
	$\mathbb{E}[D_i]$(sec)	120.8	47.16	16.03	9.094	7.367	<0.1

and the buffer size K_i (see also Table 5). Firstly, Figure 10 [1] and Table 5 show that the estimated arrival delay dramatically increases until 2483 s in the airspace $i = 1$ when we assume an arrival rate of 130% λ_i. This large amount of delay would be hardly manageable in practice. The most remarkable increase is estimated in the airspace $i = 1$ is 58.93 s and 179.8 s for 110%λ_i and 120%λ_i, respectively. Moreover, large delays are estimated in the case of airspace $i = 2$ with 20.10 s and 39.12 s for 110%λ_i and 120%λ_i, respectively. This means that approximately 40 s and 140 s of arrival delays occur between the range of circles of radii 20 NM and 40 NM, respectively.

5. Aircraft arrival control strategies under increasing arrival traffic

5.1. Exploring tactical arrival control strategies to limit arrival delay under increasing arrival traffic

As shown in section 4.3, by applying the $M/G/c/K$ queuing model for aircraft arrivals, we show that the arrival delay time is expected to increase in the future, along with increased traffic and current tactical control strategies, especially in the airspace up to 40 NM around the airport. To mitigate the impact of increasing air traffic, conventionally, two improvements have been discussed: the first is increasing the airspace capacity and runway throughput, and the second is controlling the arrival delay time in farther airspace.

In this section, we clarify the effectiveness of these two different strategies through the $M/G/c/K$ modeling approach. In section 5.2, we analyze the impact of the first strategy, i.e., increasing the capacity with 20% more than the current situation for the airspace up to 300 NM around the airport. In section 5.3, we analyze the impact of the second strategy, i.e., reducing the service time in the airspace $i = 1$ and increasing the service time in the airspace $i = 6$ while keeping the same total service time. This means that we request a shorter flight time in the airspace $i = 1$, close to the airport, and a longer flight time in the airspace $i = 6$, farther from the airport.

5.2. Increasing airspace capacity

We model an increase in the airspace capacity and runway throughput by increasing c_i and λ_i, $i \in \{1,2,\ldots,6\}$, in the proposed $M/G/c/K$ queuing model. Increasing the airspace capacity c_i means that more aircraft will be allowed to fly in an assigned airspace $i, i \in \{1,2,\ldots,6\}$. In this section, we analyze the impact of increasing the airspace capacity with 10% and 20% in each airspace $i, 1 \le i \le 6$, while assuming an increased arrival traffic rate with 10%, 20%, and 30% relative to the current air traffic.

Figure 11 and Tables 6 and 7 show the results for the estimated arrival delay $\mathbb{E}[D_i]$ for a given c_i, arrival rate λ_i, and estimated parameter values K_i to ensure $p_{Ki} < 0.01$, $i \in \{1,2,\ldots,6\}$. As expected, the results show that by increasing c_i, the expected arrival delay $\mathbb{E}[D_i]$ dramatically decreases, especially in the airspace $i = 1$ and $i = 2$. For instance, for airspace $i = 1$ and assuming an aircraft arrival rate of 120%λ_1, an arrival control strategy with an increase of 20% of the capacity c_1 results in an expected arrival delay of 8.715 s (see Table 7). However, assuming an aircraft arrival rate of 120%λ_1 for the airspace $i = 1$, keeping the current capacity c_i, results in an expected arrival delay of 179.8 s (see Table 5) . Thus, even when assuming an arrival rate of 120%λ_1 for airspace $i = 1$, approximately 3 min of arrival delay is mitigated by increasing c_1 by 20%. This 20% increase in c_1 is equivalent to increasing the number of aircraft by 1 in the airspace between the concentric circles around the airport (see Figure 5) of radii 20 NM and 40 NM (see Table 5 and Table 7).

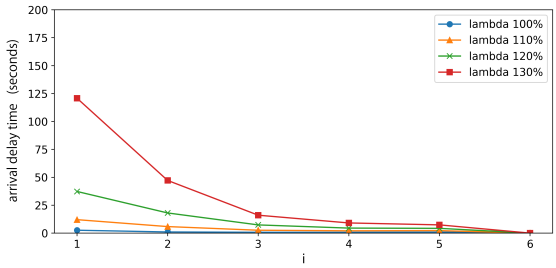

[1] Increased arrival delay time with 110%c_i and the arrival rates as 100%λ_i, 110%λ_i, 120%λ_i, and 130%λ_i.

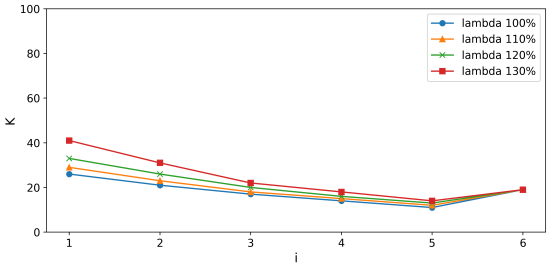

[2] Minimum buffer size K_i estimation for 110%c_i such that $p_k < 0.01$.

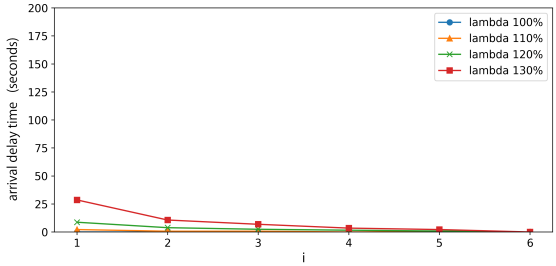

[3] Increased arrival delay time given 120%c_i and arrival rates 100%λ_i, 110%λ_i, 120%λ_i, and 130%λ_i.

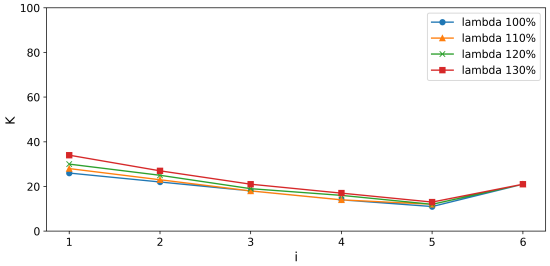

[4] Minimum buffer size K_i estimated under 120%c_i such that $p_k < 0.01$.

Figure 11: Estimating arrival delay time and minimum required buffer size under increased airspace capacity.

5.3. *Adjusting aircraft flight time*

One other means to limit the arrival time delay is to reduce the service time $\mathbb{E}[B_i]$, which is equivalent to reducing the flight time of the aircraft in an assigned airspace $i, 1 \le i \le 6$. In (7), it was proposed that an efficient arrival delay management strategy in the en-route airspace is located farther away from the destination airport than the terminal airspace surrounding the airport. In the same line, this section compares the impact of service time adjustments. In particular, we assess the strategy when a part of the service time in the airspace $i = 1$ shifts to the airspace $i = 6$. We compare the results obtained by this service time adjustments strategy against the strategy when we increase the airspace capacity $c_i, i \in \{1, 6\}$ with 10% and 20%, as discussed in section 5.2. The total service time in the airspace $i = 1$ and $i = 6$ are the same both in the case of the service time adjustment strategy, as well as in the case of the capacity increase strategy.

We consider three different service time adjustment control strategies such that a part of the service time, i.e.,

Table 7: Expected arrival delay time $\mathbb{E}[D_i]$ given 120%c_i and the estimated minimum required buffer size K_i such that $p_{K_i} < 0.01, 1 \le i \le 6$.

i		**1 (20-150NM)**	**2 (40-150NM)**	**3 (60-150NM)**	**4 (80-150NM)**	**5 (100-150NM)**	**6 (150-300NM)**
c_i		**24**	**20**	**15**	**12**	**9**	**19**
λ_i	K_i	25	21	16	13	10	20
	$\mathbb{E}[D_i]$ (sec)	<0.1	<0.1	<0.1	<0.1	<0.1	<0.1
110%λ_i	K_i	27	22	17	13	11	20
	$\mathbb{E}[D_i]$ (sec)	2.173	0.6792	0.6973	0.0	0.5260	<0.1
120%λ_i	K_i	29	24	18	15	11	20
	$\mathbb{E}[D_i]$ (sec)	8.715	3.847	2.423	1.600	0.8396	<0.1
130%λ_i	K_i	33	26	20	16	12	20
	$\mathbb{E}[D_i]$ (sec)	28.61	10.68	6.876	3.458	2.169	<0.1

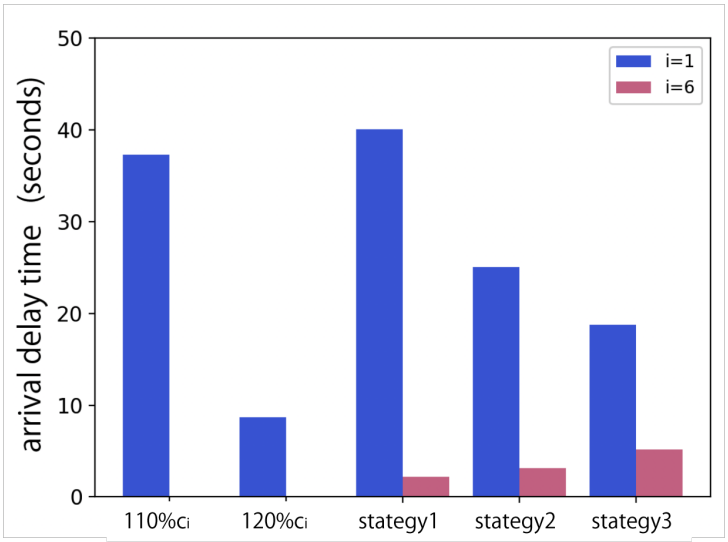

Figure 12: Comparing arrival delay time corresponding to $110\%c_i$, $120\%c_i$, and three arrival strategies.

Table 8: Aircraft arrival control strategies by adjusting the service time in the airspace $i, i \in \{1,6\}$.

Airspace i	i=1 (20-150NM)	i=6 (150-300NM)
strategy 1	$\mathbb{E}[B_1] - 100$sec	$\mathbb{E}[B_6] + 100$sec
strategy 2	$\mathbb{E}[B_1] - 150$sec	$\mathbb{E}[B_6] + 150$sec
strategy 3	$\mathbb{E}[B_1] - 180$sec	$\mathbb{E}[B_6] + 180$sec

the aircraft flight time, is shifted from the airspace $i = 1$ to $i = 6$ (see Table 8). For Strategy 1, we reduce the mean service time $\mathbb{E}[B_i]$ by 100 s in the airspace $i = 1$, and increase the service time in the airspace $i = 6$ by 100 s, while maintaining the airspace capacity $c_i, i \in \{1,6\}$ currently in use (see also Table 3). Similarly, for strategies 2 and 3, we shift 150 s and 180 s from airspace $i = 1$ to airspace $i = 6$, respectively.

Figure 12 shows the estimated arrival delay $\mathbb{E}[D_i]$ in the airspace $i = 1$ and $i = 6$ when assuming the arrival control strategies 1, 2, 3, and for the case when the capacity c_i of the airspace $i, i \in \{1,6\}$ increases with 10% and 20% compared with the current situation, i.e., we consider $110\%c_i$ and $120\%c_i$. The results show that strategies 1, 2, and 3 successfully transfer the arrival delay time from the airspace $i = 1$ to $i = 6$. However, the most effective strategy to minimize the arrival delay is to increase the airspace capacity by 20% ($120\%c_i$ in Figure 12). Although the optimizing service time in each airspace i needs further analysis, these results contribute to prioritizing future strategies on improving air traffic management systems to limit arrival delay while allowing an increase in the air traffic volume.

6. Discussion

Our proposed queue-based modeling approach clarifies that the most efficient solution to mitigate the arrival delay is to increase the airspace capacity, especially in the airspace $i = 1$ and $i = 2$, rather than adjusting the flight time (service time) of the arriving aircraft. This section discusses the implications of the outcomes for the air traffic operations.

Increasing the airspace capacity c_1 by 10% in the airspace area $i = 1$ reduces the arrival delay by 12.18 s when the arrival traffic rate remains the same as in the case of the current operations, i.e., $100\%\lambda_1 = 30$ arrivals per hour, and 46.89 s when the arrival traffic volume increased by 10% ($110\%\lambda_1 = 33$ arrivals per hour), while maintaining the current airspace capacity c_1 (see Table 6). Increasing the airspace capacity with 10% ($110\%c_1$) is equivalent to

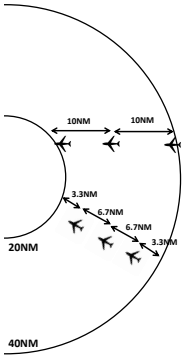

(a) Three in-trail aircraft separations under the current airspace capacity.

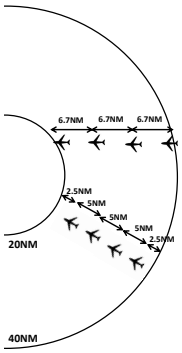

(b) Four in-trail aircraft separations under increased airspace capacity.

Figure 13: Three and four in-trail aircraft separations in the airspace 20 to 40 NM radii around the airport.

allowing one more aircraft in the airspace between the circles with radii 20 NM and 40 NM around the airport (see Table 5 and 6).

Increasing the airspace capacity by 20% (120%c_1) in the airspace area $i = 1$ relative to the current situation reduces the arrival delay by 171.1 s when the arrival traffic rate increases by 20% (120%λ_i) (see Table 7). Increasing the airspace capacity by 20% (120%c_i) relative to the current situation is equivalent to allowing two more aircraft in the airspace between the circles around the airport with radii 20 NM and 60 NM as follows: one aircraft between the circles with radii 20 NM and 40 NM and the other between the circles with radii 40 NM and 60 NM around the airport(see Tables 5 and 7).

In practice, increasing one aircraft in the airspace between the circles around the airport with radii 20 NM and 40 NM, where currently the capacity is, on average, three aircraft (see Table 5), means that a total of four aircraft are allowed to fly in this airspace. If only three aircraft follow in-trail while keeping the same spacing distance between 20 NM and 40 NM around the airport, the mean aircraft separation is estimated to be between 6.7 NM and 10 NM (see Figure 13a). If all the four aircraft follow in-trail, the mean aircraft separation is between 5 NM and 6.7 NM (see Figure 13b). In both the cases, the resulting aircraft separations satisfy the current radar-separation minimum of 5 NM. This means that increasing the airspace capacity by 1 more aircraft in the airspace 20–40 NM radii around the airport is currently a feasible strategy.

In the future, it is expected that the minimum separation will be reduced from 5NM to 3–5 NM as a result of implementing new separation standards. This will, in turn, result in an increase in the capacity, which we showed in our results. This is the most efficient strategy with respect to arrival delays. Moreover, air traffic controllers make use of a large margin for the minimum separation distance for safety reasons. In the future, increasing the level of automation support will contribute to the reduction of these safety margins, as shown in (3). In turn, this will result in a reduction of the separation minima below 5 NM, which again, will support an increase in the airspace capacity close to the airport.

This paper clarifies that the most delay-efficient strategy is to increase the airspace capacity up to 60 NM around the airport. This result supports the design of Extended Arrival Management (E-AMAN) system, which is one of the main means of automation support for air traffic controllers.

7. Conclusions

This paper proposes a novel queue-based modeling approach for aircraft arrivals at an airport and analyzes the strategies for air traffic tactical control that can mitigate arrival delays while allowing future increasing air traffic volumes. Our modeling approach is motivated by a data-driven analysis of actual flight plans and radar data corresponding to the arrival traffic in 2016 and 2017 at Tokyo International Airport. Our analysis estimates the arrival delays under increasing arrival rates and indicates that the most delay-efficient arrival tactical control strategy is to increase airspace capacity close to the arrival airport. In particular, allowing one or two additional

aircraft in the airspace within approximately 60 NM around the airport significantly reduces the arrival delays even in the case when the arrival rate increased up to 20% more than the current operations.

Our proposed approach provides support to the decision-making process of prioritizing tactical control strategies under various traffic conditions, i.e., providing support for introducing new operational procedures, designing route structures, introducing automation support for controllers. As future work, we plan to develop arrival optimization models for aircraft arrivals at an airport under increased traffic volumes such that arrival delays are minimized.

8. Acknowledgements

This research was conducted under CARATS initiatives supported by the Civil Aviation Bureau, Ministry of Land, Infrastructure, Transport and Tourism, Japan, as the "Studies on the Extended Arrival Management." This research was also supported by the Ministry of Education, Culture, Sports, Science and Technology, Japan, as the "Post-K Computer Exploratory Challenge" (Exploratory Challenge 2: Construction of Models for Interaction Among Multiple Socioeconomic Phenomena, Model Development and its Applications for Enabling Robust and Optimized Social Transportation Systems). (Project ID: hp180188).

Reference

[1] Passenger traffic 2016 final (annual). *Airports Council International (ACI), [online], 1st January*, 2018.
[2] Ivo Adan and Jacques Resing. Queuing systems. 2015.
[3] Doug Arbuckle. Interval management application. *ICAO Aircraft Surveillance Applications Workshop, March*, 2017.
[4] Nicole Bäuerle, O Engelhardt-Funke, and Michael Kolonko. On the waiting time of arriving aircrafts and the capacity of airports with one or two runways. *European Journal of Operational Research*, 177(2):1180–1196, 2007.
[5] M.A. Bolender and G.L. Slater. Evaluation of scheduling methods for multiple runways. *Journal of Aircraft*, 37(3):410–416, 2000.
[6] Long Dou, Johnson Jesse, Gaier Eric M, and Kostiuk Peter F. Modeling air traffic management technologies with a queuing network model of the national airspace system. *NASA Langley Technical Report Server*, 1999.
[7] Heinz Erzberger and Eri Itoh. Design principles and algorithms for air traffic arrival scheduling. *NASA/TP-2014-218302*, 2014.
[8] European Commission. Cross border sesar trials for enhanced arrival management: Periodic reporting for period 1 - pj25 xstream, https://cordis.europa.eu/project/rcn/207235/reporting/en. 2017.
[9] Federal Aviation Administration (FAA). Nextgen portfolio - time-based flow management, https://www.faa.gov/nextgen/snapshots/portfolios/?portfolioid=1 2017.
[10] Nacira Guerouahane, Djamil Aissani, Nadir Farhi, and Louiza Bouallouche-Medjkoune. M/G/c/c state dependent queuing model for a road traffic system of two sections in tandem. *Computers & Operations Research*, 87:98–106, 2017.
[11] Frederick Hillier. *Introduction to Operations Research*. Tata McGraw-Hill Education, 2012.
[12] International Civil Aviation Organization. Long-term traffic forecasts passenger and cargo. 2016.
[13] International Civil Aviation Organization. Long range ATFM concept trials. *The 8th Meeting of the ICAO Asia/Pacific Air Traffic Flow Management Steering Group (ATFMSG/8), May 2018, https://www.icao.int/APAC/Meetings/2018*, 2018.
[14] E Itoh, M Brown, A Senoguchi, N Wickramasinghe, and S Fukushima. Future arrival management collaborating with trajectory-based operations. In *Air Traffic Management and Systems II*, pages 137–156. Springer, 2017.
[15] Eri Itoh and Mihaela Mitici. Queue-based modeling of the aircraft arrival process at a single airport. *Aerospace*, 6(10):103, 2019.
[16] Eri Itoh and Mihaela Mitici. Evaluating the impact of new aircraft separation minima on available airspace capacity and arrival delay. *The Aeronautical Journal*, 124(1274):447–471, 2020.
[17] John Little. A proof for the queuing formula. *Operations Research*, 9(3):383–387, 1961.
[18] Khalidur Rahman, Noraida Abdul Ghani, Anton Abdulbasah Kamil, Adli Mustafa, and Md Ahmed Kabir Chowdhury. An M/M/c/K state-dependent model for pedestrian flow control and design of facilities. *PLoS one, e0133229*, 10(7), 2015.
[19] Robert C. Rue and Matthew Rosenshine. The application of semi-Markov decision processes to queuing of aircraft for landing at an airport. *Transportation Science*, 19(2):154–172, 1985.
[20] Jane Thipphavong, Jaewoo Jung, Harry Swenson, Lynne Martin, Melody Lin, and Jimmy Nguyen. Evaluation of the terminal sequencing and spacing system for performance-based navigation arrivals. In *2013 IEEE/AIAA 32nd Digital Avionics Systems Conference (DASC)*, 2013.
[21] Paul Van Tulder. Flight deck interval management flight test final report. *NASA/CR-2017-219626, June 2017*, 2017.